SANDIA REPORT

SAND2005-7005
Unlimited Release
Printed July 2006

Basin Amplification of Seismic Waves in the City of Pahrump, Nevada

Robert E. Abbott

Prepared by
Sandia National Laboratories
Albuquerque, New Mexico 87185 and Livermore, California 94550

Sandia is a multiprogram laboratory operated by Sandia Corporation,
a Lockheed Martin Company, for the United States Department of Energy's
National Nuclear Security Administration under Contract DE-AC04-94-AL85000.

Approved for public release; further dissemination unlimited.

Sandia National Laboratories

Issued by Sandia National Laboratories, operated for the United States Department of Energy by Sandia Corporation.

NOTICE: This report was prepared as an account of work sponsored by an agency of the United States Government. Neither the United States Government, nor any agency thereof, nor any of their employees, nor any of their contractors, subcontractors, or their employees, make any warranty, express or implied, or assume any legal liability or responsibility for the accuracy, completeness, or usefulness of any information, apparatus, product, or process disclosed, or represent that its use would not infringe privately owned rights. Reference herein to any specific commercial product, process, or service by trade name, trademark, manufacturer, or otherwise, does not necessarily constitute or imply its endorsement, recommendation, or favoring by the United States Government, any agency thereof, or any of their contractors or subcontractors. The views and opinions expressed herein do not necessarily state or reflect those of the United States Government, any agency thereof, or any of their contractors.

Printed in the United States of America. This report has been reproduced directly from the best available copy.

Available to DOE and DOE contractors from
U.S. Department of Energy
Office of Scientific and Technical Information
P.O. Box 62
Oak Ridge, TN 37831

Telephone: (865) 576-8401
Facsimile: (865) 576-5728
E-Mail: reports@adonis.osti.gov
Online ordering: http://www.osti.gov/bridge

Available to the public from
U.S. Department of Commerce
National Technical Information Service
5285 Port Royal Rd
Springfield, VA 22161

Telephone: (800) 553-6847
Facsimile: (703) 605-6900
E-Mail: orders@ntis.fedworld.gov
Online ordering: http://www.ntis.gov/help/ordermethods.asp?loc=7-4-0#online

SAND2005-7005
Unlimited Release
Printed July 2006

Basin Amplification of Seismic Waves in the City of Pahrump, Nevada

Robert E. Abbott
Solid Dynamics and Energetic Experiments Department
Sandia National Laboratories
P.O. Box 5800
Albuquerque, NM 87185-1168
reabbot@sandia.gov

Abstract

Sedimentary basins can increase the magnitude and extend the duration of seismic shaking. This potential for seismic amplification is investigated for Pahrump Valley, Nevada-California. The Pahrump Valley is located approximately 50 km northwest of Las Vegas and 75 km south of the Nevada Test Site. Gravity data suggest that the city of Pahrump sits atop a narrow, approximately 5 km deep sub-basin within the valley. The seismic amplification, or "site effect", was investigated using a combination of *in situ* velocity modeling and comparison of the waveforms and spectra of weak ground motion recorded in the city of Pahrump, Nevada, and those recorded in the nearby mountains. Resulting spectral ratios indicate seismic amplification factors of 3-6 over the deepest portion of Pahrump Valley. This amplification predominately occurs at 2-2.5 Hz. Amplification over the deep sub-basin is lower than amplification at the sub-basin edge, location of the John Blume and Associates PAHA seismic station, which recorded many underground nuclear tests at the Nevada Test Site. A comprehensive analysis of basin amplification for the city of Pahrump should include 3-D basin modeling, due to the extreme basement topography of the Pahrump Valley.

Acknowledgments

Thanks to Elida Vargas, Jody Maer, Paul Hernandez, Jolie Coleman, and Ivars Gals, all of Pahrump, NV, for allowing us to site stations on their property. Dr. Artie Rodgers and Lawrence Livermore National Laboratory supplied the PAHA UGT data. Most fieldwork was performed by Robert White and Michael O'Connor of Bechtel Nevada. *In situ* velocity characterization fieldwork was performed by University of Nevada, Reno, students Tiana Rasmussen, Karalyn Heath, and Sean Warren.

Contents

Introduction 9

Motivation 9

Geologic Setting 9

Method 10

Standard Spectral Ratio Technique 11

Horizontal-to-Vertical Spectral Ratio Technique 11

In Situ Velocity Characterization and Modeling 12

Results 12

Earthquake and Nuclear Event Data 12

Seismic Velocity Data 13

Spectra 16

Experimental and Synthetic Spectral Ratios 18

Discussion 18

Conclusions 22

References 24

List of Figures

1 Basemap and Stations 9

2 Seismometers 13

3 Event Map 15

4 Sample Earthquake 16

5 Sample Slowness-Frequency Plot 17

6 Dispersion Curves 17

7 Depth Profiles 17

8 Raw Spectra 18

9 Standard Spectral Ratios 19

10 H/V Spectral Ratios and Synthetics 20

List of Tables

1 Recorded Earthquakes 14

2 Nuclear test data from legacy PAHA station 15

3 *In Situ* Velocity Summary 16

4 NEHERP Site Categories 17

Introduction

Motivation

The goal of this report is to seek the seismic site effect for Pahrump, Nevada, so that the seismic hazard represented by any future underground nuclear tests at the Nevada Test Site (NTS) can be found beforehand. Pahrump is located in southern Nevada, approximately 80 km northwest of Las Vegas and 75 km south of the NTS (Figure 1, inset). The city has recently seen dramatic growth. From the year 1990 to the year 2000 U.S. census, the population has increased by over 230 percent and the growth rate has only increased since then (`http://factfinder.census.gov`). In addition, as of 2000, over 60 percent of all homes were built between the two census periods. This is significant as most of these homes have never been subject to ground motions from previous underground nuclear tests (UGTs) at the NTS (the most recent UGT was conducted in 1992). Previous seismic ground motion recordings from pre-1992 UGTs are only available for the legacy John Blume and Associates PAHA station (Figure 1). As this station is on the fringe of the deep sub-basin, it is possible that analysis of these recordings alone underestimate the potential hazard. It is therefore desirable to collect new data over the deepest portion of the valley.

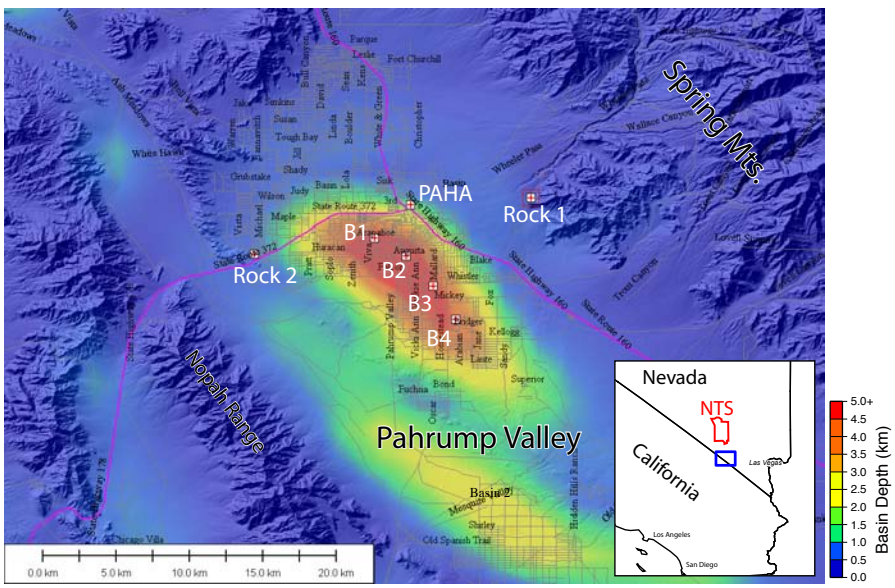

Figure 1: Location map for Pahrump, Nevada. Inset blue box is map extent. Colors represent basin depth from Jachens and Moring (1990). Red crosses indicate seismic sensors deployed for this study (B1-B4, Rock 1, Rock 2) or deployed prior to 1992 (PAHA).

Geologic Setting

The city of Pahrump is located in the Pahrump Valley, an alluvial basin near the southern Nevada-California border. Regional extension in the middle to late Cenozoic produced the

current topography (Wernicke et al., 1988). Basin fill consists of fine-grained sediments eroded from the surrounding mountain ranges. The bounding mountain ranges (Spring Mts., northeast and east; Montgomery Mts., northwest; Kingston Range, southwest; and Nopah Range, west) consist primarily of late Proterozoic and Paleozoic carbonate and other sedimentary rocks with some localized intrusive rocks (Stewart and Carlson, 1978). The basin depth inferred from gravity data is generally less than 1 km outside of two narrow sub-basins, where depths can reach in excess of 4.5 km (Jachens and Moring, 1990). The deeper of the two sub-basins is directly overlain by portions of the City of Pahrump. Splitting the sub-basins is a large, right-lateral strike-slip fault, alternatively called the Pahrump Valley Fault Zone or the Stateline Fault. Shields et al. (1998) speculate that a magnitude 7 earthquake may be possible along this reach of the Pahrump Valley Fault Zone. If true, the fault would represent the greatest seismic hazard for Pahrump, and probably for the greater Las Vegas area, as well.

Method

The recorded ground motion of a seismic event is a convolution of a number of factors. Four major influences on recorded data are source, propagation, instrumental, and site effects.

Source effects manifest themselves at or near the hypocenter of the seismic event. They reflect such properties as rupture mechanics (fault orientation, fault size, rupture direction, explosive yield, etc.), and the physical properties of the earth at the source, such as rock strength.

Propagation effects are caused by the geometry of the earth's structure between the source and the recording site. These effects include refraction, reflection, scattering, and absorption, among others.

Instrumental effects are caused by the instruments used to record the motion. Both the seismometer (the instrument sensitive to ground motion) and the seismograph (the digitizer that converts the output of the seismometer to 1's and 0's) act as a filter.

Site effects are caused by the response of the earth near the recording site. Examples of site effects include subsurface focusing of seismic waves at basin boundaries, shaking due to surface waves created at basin boundaries, and resonance modes in layers of low-velocity sediments (Field, 2000). There is no clear definition of "near station" in determining what is a site effect and what is not. For instance, subsurface focusing may be considered a propagation effect, depending on the goals of the study. Here, I define site effect as any phenomena that is the result of seismic waves interacting with geology within the the confines of the Pahrump Valley.

The goal of this paper is to quantify this last contribution (the site effect) at selected locations in the city of Pahrump, Nevada. In the process, I will try to account for, and eliminate, effects from the other three contributing factors. To do this, I will use two spectral ratio techniques: "standard" and "horizontal-to-vertical". I will also measure the *in situ* seismic shear-wave velocity at the locations of our seismic stations and create 1-D synthetic spectral ratios for comparison. The methodology of the three techniques is briefly discussed below.

Standard Spectral Ratio Technique

Define the Fourier spectra A_{ij} of ground motion at frequency f for earthquake i at site j as

$$A_{ij}(f) = S_i(f)P_{ij}(f)I_j(f)R_j(f) + n_j(f)I_j(f)R_j(f) \tag{1}$$

where $S_i(f)$ is the source spectra, $P_{ij}(f)$ is the propagation operator, $I_j(f)$ is the instrument operator, $R_j(f)$ is the site operator, and $n_j(f)$ is uncorrelated (seismic) noise at site j. For the same earthquake recorded at site k, close to site i, equation (1) becomes

$$A_{ik}(f) = S_i(f)P_{ik}(f)I_k(f)R_k(f) + n_k(f)I_k(f)R_k(f). \tag{2}$$

Assuming the seismic noise spectra is dominated by the earthquake spectra at the frequencies of interest, ratioing (1) and (2) results in

$$\frac{A_{ij}(f)}{A_{ik}(f)} = \frac{S_i(f)P_{ij}(f)I_j(f)R_j(f)}{S_i(f)P_{ik}(f)I_k(f)R_k(f)} \approx \frac{R_j(f)}{R_k(f)} \tag{3}$$

as the source spectra and instrument effects cancel exactly (if the instrument responses are known) and given the assumption that differences in propagation are minimal due to the close proximity of the recording stations relative to the distant event. The term that remains $\frac{R_j(f)}{R_k(f)}$ is the site effect of site j relative to site k. Borcherdt (1970) first used this technique (called "standard spectral ratio", or SR, here). In Borcherdt (1970), spectra recorded at basin sites in the San Francisco Bay Area were ratioed with spectra recorded on nearby bedrock. Marked differences were found, with ground motion being up to ten times greater at sedimentary sites. Bedrock sites are generally assumed to be free from site effects (i.e., $R_k(f) \approx 1$ in equation (3)), therefore the differences in spectra can be attributed to the site effect of the basin site. However, there is ample evidence that not all "rock" sites make good reference sites (e.g., Steidl et al. (1996); Humphrey Jr and Anderson (1992); Tucker et al. (1984)). Weathered layers, topographic irregularities, and rock inhomogeneity can result in rock site variability.

Horizontal-to-Vertical Spectral Ratio Technique

In contrast to the standard spectral ratio technique (SR), which requires two stations (a reference station and the station of interest), the horizontal-to-vertical spectral ratio (HVSR) technique only requires one. This makes this technique highly desirable if a suitable reference station cannot be found, as is the case when bedrock is too distant or noise characteristics at one of the sites are unfavorable. The technique relies on the assumption that the vertical component of seismic motion is relatively insensitive to site effects. In essence, the vertical component closely mirrors the ground motion that would have been recorded on a (co-located) rock station, in theory, removing the necessity of the reference station. One has to be aware that some energy can be scattered at layer boundaries from the horizontal into the the vertical orientation, however.

The technique was pioneered by Nakmura (1989), using microtremors (ambient Earth noise) as the source. Castro et al. (1997) tested the technique on energetic S-waves from earthquakes and found that as long as significant Rayleigh-wave energy is not in the time window, satisfactory agreement with other techniques were achieved. Generally, studies comparing the HVSR and SR techniques have mixed results. For some, (e.g., Lermo and Chavez-Garcia (1993); Castro et al. (1997)), both frequencies and amplitudes are consistent. For others, only the fundamental resonance frequency, but not amplitude (e.g., Field and Jacob (1995); Field (1996); Lachet et al. (1996)), is correctly predicted.

In Situ Velocity Characterization and Modeling

The site-specific distribution of layered soils with different physical properties can have a great effect on seismic shaking (e.g., Idriss and Seed (1968)). Modeling the effects of soils at sites that can be approximated by 1-D geometries (vertically changing, but horizontally homogeneous), is common. In general, one needs to know the gross characteristics of the soil beneath the site, whether by examining drill cores, conducting penetrability experiments, or local seismic experiments. Once the gross characteristics are found, it is often necessary to consult tables of average properties to complete the analysis. `SHAKE` was one of the first computer programs to model the site-effects of stacks of soils (Schnabel et al., 1972). `SHAKE` models the effect of horizontally stacked soils of infinite extent over a basal rock formation on vertically-incident, planar shear waves. In this way, it is very analogous to the HVSR technique. The soil is completely described by layer thickness, density, shear modulus, and damping ratio (which measures the soil's attenuative properties). For this study, the program `EERA` (**E**quivalent-Linear **E**arthquake Site **R**esponse **A**nalyses of Layered Deposits), a modern implementation of the `SHAKE` methodology, was used (Bardet et al., 2000).

The Refraction-Microtremor (ReMi) method of (Louie, 2001) was used to find the necessary soil parameters. Data collection commonly consists of placing 12 to 24 seismic sensors in a line at the site, at 5-20 meter intervals. Then, several minutes of either ambient noise (microtremor) or an active seismic source is recorded. The dispersive properties of surface waves in the data are used to to create a model of shear-wave velocity and density vs. depth. The shear-wave velocity is used to calculate shear modulus for input into `EERA`, leaving only damping ratio to be estimated from table values.

Results

Earthquake and Nuclear Event Data

The seismic network consisted of six matched and calibrated three-component digital stations temporarily placed in and around the city of Pahrump, Nevada. The six stations used shallowly buried Teledyne-Geotech GS-13 seismometers (1 Hz resonance, 2000 V/cm/sec), recorded at 50 samples per second (Figure 2). Four stations were deployed over the deepest portion of the basin and two stations were deployed on bedrock (B1–B4 and Rock 1 & 2 on Figure 1).

Figure 2: Three Teledyne-Geotech GS-13 seismometers before burial (one vertical, and two horizontal).

From March to November 2004, the seismic network recorded 60 earthquakes with sufficient signal-to-noise ratio ($\frac{S}{n} \geq 5$ for pre-event noise at given frequencies) to be included for analysis (Figure 3; Table 1). Figure 4 shows a sample event recorded on a basin and rock site. The earthquakes ranged in magnitude from $M_L = 2.1$ to $M_L = 6$. In addition to the earthquake data, I have ground motion from eleven UGTs (Table 2) at the Nevada Test Site recorded at the legacy John Blume and Associates PAHA station (Figure 1).

Seismic Velocity Data

At each of the six seismic stations I measured the shear-wave velocity structure using the method of Louie (2001). Measurements were made using RefTek RT-13 "Texan" seismic recorders with 4.5 Hz single-component geophones. In general, the recording geometry consisted of 20 recorders, spaced linearly at 15-m intervals. Therefore, the measured velocity profile represents the average velocity beneath the 300-m long array. Figure 5 shows a sample slowness-frequency plot from data recorded at a basin site. Data quality was good for all the basin sites. However, data quality at rock sites was poor. For those sites, I estimated S-wave velocity from P-wave first arrival picks in the time domain, assuming a Poisson's ratio of 0.5. Also, I assumed velocity to be constant with depth in the upper 60 meters.

Figures 6 and 7, summarize the dispersion curves and resultant velocity profiles, respectively.

Table 1: Earthquakes recorded, March–November, 2004. A '•' indicates that the given event for that station was used in the analysis.

Event	Jul. Day	UTM	Lat.	Long.	Mag.	B1	B2	B3	B4	R1	R2
1	77	23:53:04	35.499	-121.283	4.5			•		•	•
2	79	01:09:23	34.308	-116.933	3.5			•		•	•
3	80	04:55:37	33.513	-116.576	3.1			•		•	•
4	83	21:30:56	36.576	-114.965	2.6	•		•	•	•	•
5	88	07:20:02	36.153	-118.134	4.0	•		•	•	•	•
6	91	04:57:35	36.179	-118.159	3.1	•	•	•	•	•	•
7	93	22:51:51	35.347	-117.193	3.2	•	•	•	•	•	•
8	96	04:44:46	35.638	-117.561	2.7	•	•	•		•	•
9	96	10:27:15	34.184	-116.887	2.9	•	•	•		•	•
10	111	23:30:16	35.974	-116.758	2.9		•		•	•	•
11	112	12:56:08	35.527	-116.233	2.5	•	•		•	•	•
12	117	23:26:59	36.487	-116.579	2.8	•	•	•		•	•
13	130	08:57:17	34.395	-120.022	4.4	•	•	•	•	•	•
14	137	01:29:39	37.280	-114.840	4.5	•	•	•	•	•	•
15	141	17:00:20	37.306	-114.822	3.9	•	•	•	•	•	•
16	155	08:54:45	39.330	-120.021	4.5	•	•	•	•	•	•
17	167	22:28:49	32.383	-117.847	5.3	•	•	•	•	•	•
18	181	10:20:44	36.103	-117.796	3.4	•	•	•	•	•	•
19	196	00:53:52	33.711	-116.056	4.0	•	•	•	•	•	•
20	206	12:55:19	34.380	-119.436	4.3	•	•	•	•	•	•
21	207	14:52:23	36.141	-121.131	4.4	•	•	•	•	•	•
22	223	14:17:18	37.449	-117.083	3.5	•	•	•	•	•	•
23	235	01:25:12	32.342	-115.224	4.2	•	•		•	•	•
24	236	13:22:13	34.671	-116.359	3.2	•	•	•	•	•	•
25	244	00:09:13	35.599	-117.035	3.2	•	•	•		•	•
26	259	01:46:06	36.103	-117.739	3.0			•		•	•
27	260	13:29:30	34.121	-116.403	3.6	•	•			•	•
28	263	04:51:30	37.983	-118.688	3.4		•	•		•	•
29	263	06:58:04	37.983	-118.688	3.8	•	•	•	•	•	•
30	264	16:51:05	38.028	-118.630	4.9	•	•	•	•	•	•
31	265	08:25:11	38.028	-118.630	3.6	•	•	•	•	•	•
32	272	17:15:22	35.694	-120.445	6.0	•	•	•	•	•	•
33	273	06:27:18	37.953	-118.655	3.4	•	•	•		•	•
34	273	17:10:04	35.886	-120.506	5.0	•	•	•	•	•	•
35	274	18:54:30	35.912	-120.533	5.0		•	•	•	•	•
36	275	19:22:18	37.421	-117.048	3.9	•	•	•	•	•	•
37	276	12:22:08	35.556	-120.816	4.3	•	•	•		•	•
38	283	06:39:09	36.045	-117.812	3.3	•	•	•	•	•	•
39	283	12:02:43	34.830	-118.350	3.1	•	•	•	•	•	•
40	283	03:45:49	37.964	-118.653	4.4			•		•	•
41	298	12:49:06	36.981	-115.564	2.1		•	•		•	•
42	298	13:20:33	38.026	-118.643	3.5	•	•	•		•	•
43	301	21:41:17	34.343	-116.918	3.8	•		•	•		•
44	306	14:49:49	34.725	-116.050	3.2	•		•	•	•	•

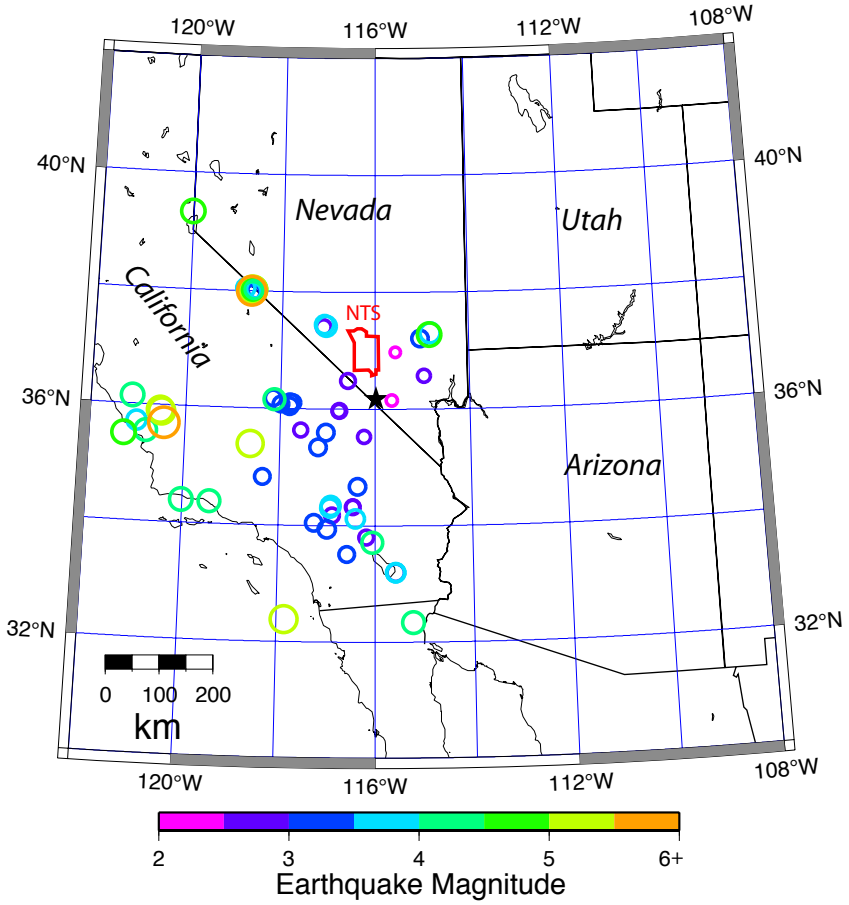

Figure 3: Earthquakes Recorded, March–November, 2004. The star represents the city of Pahrump.

Table 2: Nuclear events recorded on legacy Blume Network PAHA station. Event particulars are from Springer et al. (2002).

Event	Name	Date	UTC Time	Lat.	Long.	Yield (kt)
1	Boxcar	04/26/1968	15:00:00.07	37.295	-116.457	1300
2	Handley	03/26/1970	19:00:00.20	37.300	-116.535	> 1000
3	Muenster	01/03/1976	19:15:00.16	37.297	-116.334	200-1500
4	Fontina	02/12/1976	14:45:00.16	37.271	-116.489	200-1500
5	Jornada	01/28/1982	16:00:00.10	37.091	-116.052	139
6	Nebbiolo	06/24/1982	14:15:00.09	37.236	-116.371	20-150
7	Mundo	05/01/1984	19:05:00.09	37.106	-116.023	20-150
8	Cottage	03/23/1985	18:30:00.08	37.180	-116.090	20-150
9	Gascon	11/14/1986	16:00:00.07	37.100	-116.049	20-150
10	Bodie	12/13/1986	17:50:05.08	37.263	-116.413	20-150
11	Tahoka	08/13/1987	14:00:00.09	37.061	-116.046	20-150

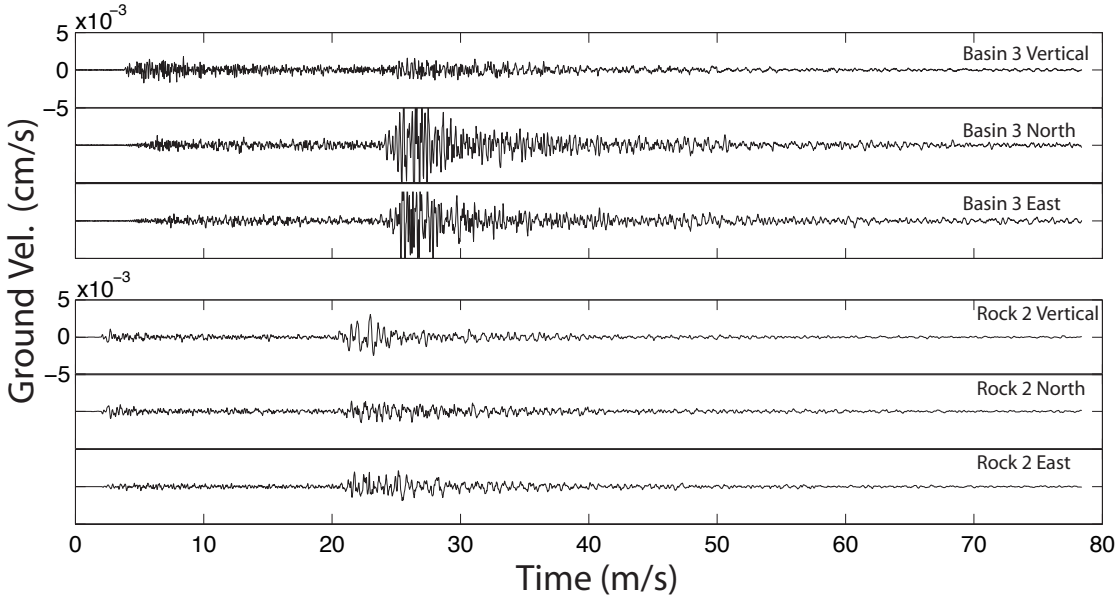

Figure 4: Magnitude 4.5 earthquake near Pioche, NV. Note the increased ground motion recorded on the basin site, relative to the rock site. The effect is much more prominent for the S arrivals (at $\approx$ 23 seconds) on the horizontal components.

Table 3: Average 30-meter velocities and NEHRP site categories for all basin sites.

Station	V_{30} **Velocity (m/s)**	**NEHRP Class**
Basin 1	352	D
Basin 2	399	C
Basin 3	299	D
Basin 4	298	D
PAHA	467	C

Under National Earthquake Hazards Reduction Program (NEHRP) guidelines, all sites are classified as type "D" or type "C" (stiff soil to very dense soil) (Tables 3 and 4). NEHRP classes are based on the average shear-wave velocity in the upper 30 meters, V_{30}. This parameter has been shown to correlate with average amplification factors. Due to this, V_{30} is used in the preparation of seismic hazard maps (e.g. (Frankel et al., 1996)) and building codes (Building Seismic Safety Council: `http://www.bssconline.org/`).

Spectra

I computed the spectra of ground velocity for each component of each station. The computed Fourier spectra is for a 5-second time window, starting one-half second before S-wave arrival. I chose this window to best contain most of the high amplitude direct S-wave energy. As pointed out in Bonilla et al. (1997) and Satoh et al. (2001), using longer times may result in better spectral resolution but the longer windows contain more energy from surface

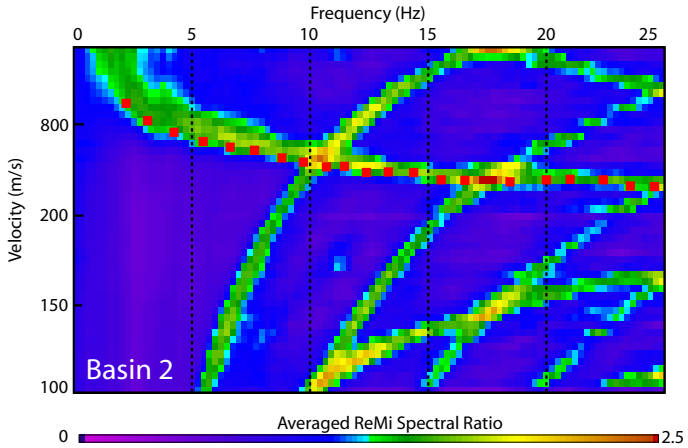

Figure 5: Slowness-Frequency plot for station B2. Red dots are picks of the Rayleigh-wave dispersion curve. This dispersion curve can be used to invert for the shear-wave velocity structure of the area sampled by the measurements, after Louie (2001). The up and to-the-right curves are FFT and data-truncation artifacts inherent to the method.

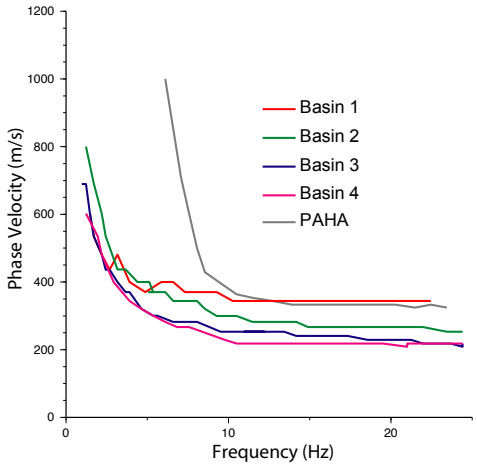

Figure 6: Surface-wave dispersion curves for all four basin sites and the legacy Blume Network site.

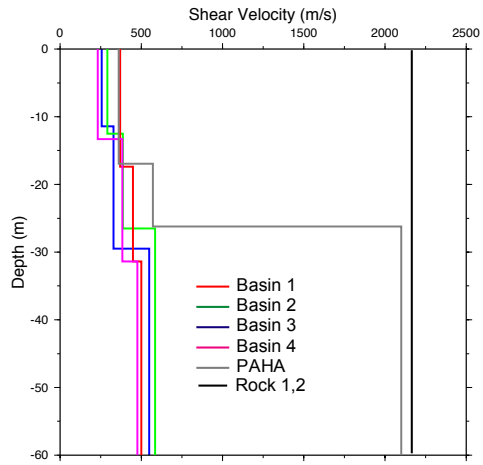

Figure 7: Shear-wave velocity structure from forward modeling of dispersion curves for each basin site

Table 4: National Earthquake Hazards Protection (NEHRP) site categories.

Category	**Description**	V_{30} **(m/s)**
A	Hard rock	> 1500
B	Rock	760-1500
C	Very dense soil, soft rock	360-760
D	Stiff soil	180-360
E	Soft soil	< 180
F	"Special" soils	n/a

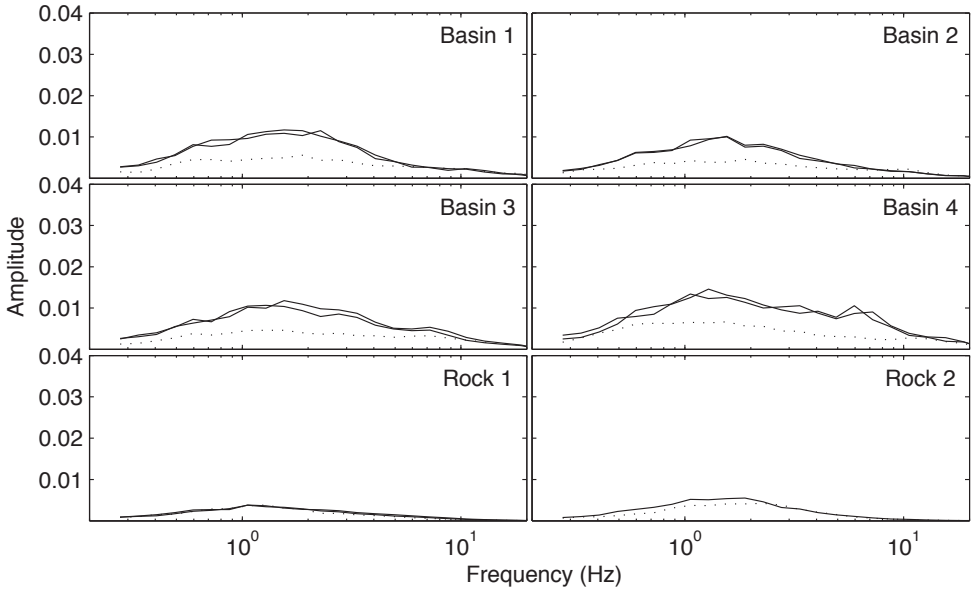

Figure 8: Raw spectra for all recording sites. Dashed lines represent the vertical spectra, solid lines represent the horizontal spectra. Note the elevated horizontal spectra at the basin sites. Data at frequencies below 0.5 Hz are suspect, due to sensitivity roll-off of the 1-Hz seismometers.

waves and other phases. For each 5-second seismogram, I removed the mean value and applied a 10% Tukey window. After Fast Fourier Transform, the two horizontal spectra for each record were averaged to form one horizontal spectrum. Logarithmically averaging the spectra of all events for each site, resulted in the spectra presented in Figure 8.

Experimental and Synthetic Spectral Ratios

I computed spectal ratios of ground motion using both the SR and HVSR methods (Figures 9 and 10). In each case, I computed the ratios separately for each event, and arithmetically averaged the individual ratios. Synthetic spectral ratios from *in situ* velocities, calculated using `EERA`, are also presented in Figure 10.

Discussion

The three methods used in this study all show that the seismic amplification over the deepest part of the Pahrump Valley is relatively slight for the frequencies studied. Maximum amplifications at the basin sites are less than 4 for all Basin sites for both the HVSR and synthetic spectral ratio methods (Figure 10). Amplifications from the standard spectral ratios will be discussed below. The resonant frequency for Basin sites 1-3 is $\approx$ 2-2.5 Hz, for both HVSR and synthetic methods. Site Basin 4 has a peak in that range, as well as an additional broad peak centered at $\approx$ 6 Hz. This peak is unexplained by the velocity models

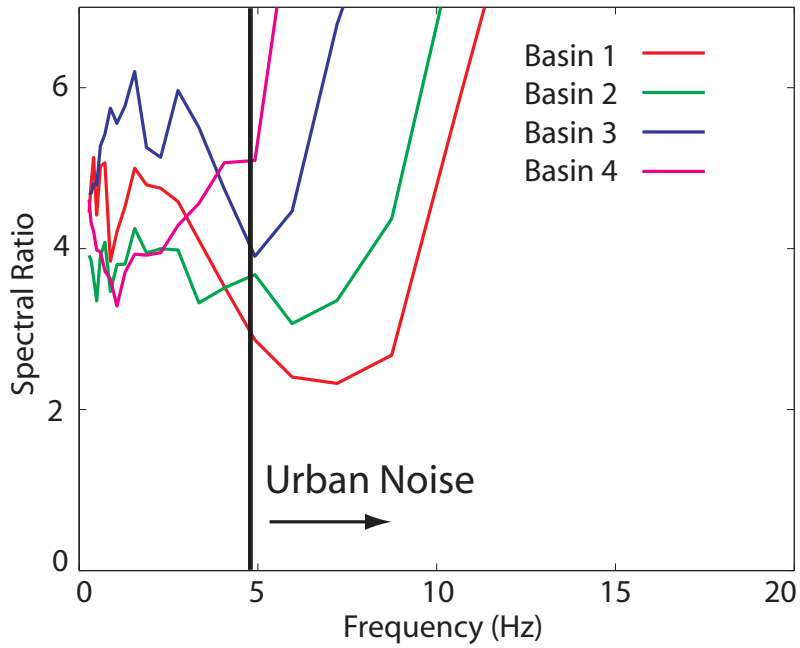

Figure 9: Ratios of the horizontal component of Basin stations 1-4, relative to station Rock 2. Above 5 Hz, urban vibrations at the basin sites overpower the earthquake spectra. See Discussion.

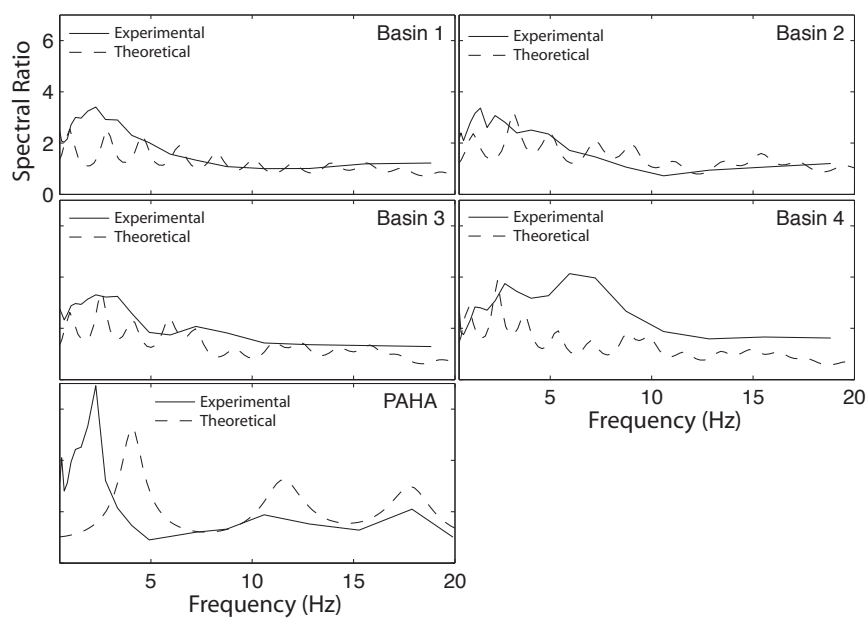

Figure 10: Single-station ratios of the horizontal component of ground motion relative to the vertical component. Also, synthetic spectral ratios generated with `EERA` from *in situ* velocity characterization (Figure 7).

and synthetics, and not reproducible by the SR technique due to noise considerations. Site PAHA, shows a slightly different character, as is to be expected since it lies on the edge of the deep sub-basin, rather than atop it. Maximum amplification is increased at PAHA, to the 6-7x range, and the resonance in the synthetic ratio shifts out to 4.75 Hz. However, the computed HVSR maximum amplification at PAHA is at approximately 2.5 Hz. This mismatch can possibly be attributed to 3-D effects, as will be discussed below. Synthetic modeling indicates that the increased hazard at this frequency range for the PAHA station is most likely caused by wave resonance at the sharp velocity discontinuity at ≈ 25 meters depth (Figure 7). The relatively smooth velocity profiles for the basin sites in Figure 7 do not result in strong resonances in this frequency range. A strong resonance probably occurs at the Basin sites due to the lower basin boundary, but it is unresolved. Basin-depth resonance frequency can be estimated by applying the standard relation for quarter-wavelength resonance, $f_{res} = \frac{1}{4}\frac{V_{avg}}{h}$, and assuming reasonable values for average velocity V_{avg}, and basin depth h. This yields resonant frequencies on the order of 0.1 Hz. This frequency is well below the frequency range of the 1 Hz GS-13s used in this study (sensitivity at 0.1 Hz is 40 dB below sensitivity at 1 Hz). By way of comparison, the same quarter-wavelength rule-of-thumb correctly predicts the 4.75 Hz resonance of the PAHA synthetic spectral ratio.

Unfortunately, the standard spectral ratios (Figure 9) are of limited use above 5 Hz, making comparisons with the other methods difficult. Above 5 Hz, urban vibrations dominate the earthquake spectra, violating the assumption of equation (1). The rock stations were located at the nearest possible rock outcrops, but these were outside the city, as seen in Figure 1. Peak amplifications are slightly higher (4-6x compared to 3-4x), for the SR method but the resonant frequencies are in close agreement ($\approx$ 2-2.5 Hz) with the HVSRs. A percentage of the increased spectral ratio amplitudes relative to the HVSR amplitudes can be attributed to the increased noise at the basin sites (noise being broadband), making the agreement between the methods quite reasonable.

The degree to which the three methods' ratios disagree can be attributed to the breakdown of the assumptions of the relative methods. The assumption of negligible noise for the SR method was noted above. Perhaps the biggest breakdown is from unaccounted for 3-D effects. As mentioned previously, sub-surface focusing of seismic waves can be a component of the site-effect. The extremely narrow and deep sub-basin that the Basin sensors overly act as a giant lens for incoming seismic waves. Although the SR and HVSR methods try to eliminate propagation and source effects on a per-event basis, a systematic bias can creep in if the earthquake back-azimuths are not uniformly distributed. Examination of Figure 3 shows that most events originate in southern to central California, with very few data coming from east and north of Pahrump. This is a natural consequence of the relative seismicity rate of the region. If the situation was reversed (i.e. more events from the north and east) the refraction at the basin bottom might differ significantly. Unfortunately, only 4 event from the east and zero from the north make testing this hypothesis impossible. The lack of events from the north is especially disappointing, as seismic hazard from UGTs is a main motivation of this report. The synthetic spectral ratio method, of course, ignores 3-D and 2-D events by assuming plane waves at zero-degree angle-of-incidence. This leads to the "ringiness" appearance of the ratios, which is seldom as pronounced in "real world" data. This character is seen, to a lesser extent, in the PAHA HVSR ratio, however (Figure 10).

Conclusions

Examination of earthquake and nuclear event data over the city of Pahrump, Nevada, has shown the seismic site effect to be relatively slight. Results from three analytical methods (horizontal-to-vertical spectral ratio, standard (reference station) spectral ratio, and *in situ* velocity characterization and 1-D modeling) are in general agreement. The sites over the deep sub-basin lie on NEHRP classification C and D soils. Amplification factors range from 3-6x, with resonant frequencies around 2 to 2.5 Hz. Amplification at frequencies below 0.5 Hz are likely to be higher, but the instrumentation used was unable to resolve this. These amplification factors are slightly less than those at the John Blume and Associates legacy PAHA station, which recorded many underground nuclear tests. The lack of 3-D modeling and scarcity of seismic events outside southern and central California are limitations of this study.

References

Bardet, J. P., Ichii, K., and Lin, C. H. EERA: A computer program for equivalent-linear earthquake site response analysis of layered soil deposits:, 2000.

Bonilla, L. F., Steidl, J. H., Lindley, G. T., Tumarkin, A. G., and Archuleta, R. J., 1997, Site amplification in the San Fernando Valley, California; variability of site-effect estimation using the s-wave, coda, and H/V methods: Bulletin of the Seismological Society of America, **87**, no. 3, 710–730.

Borcherdt, R. D., 1970, Effects of local geology on ground motion near San Francisco Bay: Bulletin of the Seismological Society of America, **60**, no. 1, 29–61.

Castro, R. R., Mucciarelli, M., Pacor, F., and Petrungaro, C., 1997, S-wave site-response estimates using horizontal-to-vertical spectral ratios: Bulletin of the Seismological Society of America, **87**, no. 1, 256–260.

Field, E. H., and Jacob, K. H., 1995, A comparison and test of various site-response estimation techniques, including three that are not reference-site dependent: Bulletin of the Seismological Society of America, **85**, no. 4, 1127–1143.

Field, E. H., 1996, Spectral amplification in a sediment-filled valley exhibiting clear basin-edge-induced waves: Bulletin of the Seismological Society of America, **86**, no. 4, 991–1005.

Field, E. H., 2000, Accounting for site effects in probabilistic seismic hazard analyses of Southern California; overview of the SCEC Phase III report: Bulletin of the Seismological Society of America, **90**, no. 6, Part B Suppl., S1–S31.

Frankel, A. D., Mueller, C. S., Barnhard, T. P., Perkins, D. M., Leyendecker, E. V., Dickman, N., Hanson, S. L., and Hopper, M. G., National seismic-hazard maps; Documentation June 1996:, Open-File Report - U. S. Geological Survey OF 96-0532, U. S. Geological Survey, 1996.

Humphrey Jr, J. R., and Anderson, J. G., 1992, Shear-wave attenuation and site response in Guerrero, Mexico: Bulletin of the Seismological Society of America, **82**, no. 4, 1622–1645.

Idriss, I. M., and Seed, H. B., 1968, Seismic response of horizontal soil layers: Proceedings of the American Society of Civil Engineers Journal of Soil Mechanics and Foundations Division, **94**, 1000–1031.

Jachens, R. C., and Moring, B. C., Maps of the thickness of Cenozoic deposits and the isostatic residual gravity over basement for Nevada:, Technical Report OF 90-0404, U. S. Geological Survey, 1990.

Lachet, C., Hatzfeld, D., Bard, P.-Y., Theodulidis, N., Papaioannou, C., and Savvaidis, A., 1996, Site effects and microzonation in the city of Thessaloniki (Greece); comparison of different approaches: Bulletin of the Seismological Society of America, **86**, no. 6, 1692–1703.

Lermo, J., and Chavez-Garcia, F. J., 1993, Site effect evaluation using spectral ratios with only one station: Bulletin of the Seismological Society of America, **83**, no. 5, 1574–1594.

Louie, J. N., 2001, Faster, better: Shear-wave velocity to 100 meters depth from refraction microtremor arrays: Bulletin of the Seismological Society of America, **91**, no. 2, 347–364.

Nakmura, Y., 1989, A method for dynamic characteristics estimation of subsurface using microtremor on the ground surface: QR Railway Technical Research Institute, **30**, no. 1.

Satoh, T., Kawase, H., and Matsushima, S., 2001, Differences between site characteristics obtained from microtremors, s-waves, p-waves, and codas: Bulletin of the seismological Society of America, **91**, no. 2, 313–344.

Schnabel, P. B., Lysmer, J., and Seed, H. B., Shake: A computer program for earthquake response analysis of horizontally layered sites:, Technical Report UCB/EERC-72/12, Earthquake Engineering Center, University of California, Berkeley, 1972.

Shields, G., Allander, K., Brigham, R., Crosbie, R., Trimble, L., Sleeman, M., Tucker, R., Zhan, H., and Louie, J. N., 1998, Shallow geophysical survey across the Pahrump Valley fault zone, California-Nevada border: Bulletin of the Seismological Society of America, **88**, no. 1, 270–275.

Springer, D. L., Pawloski, G. A., Ricca, J. L., Rohrer, R. F., and Smith, D. K., 2002, Seismic source summary for all U.S. below-surface nuclear explosions: Bulletin of the Seismological Society of America, **92**, no. 5, 1806–1840.

Steidl, J. H., Tumarkin, A. G., and Archuleta, R. J., 1996, What is a reference site?: Bulletin of the Seismological Society of America, **86**, no. 6, 1733–1748.

Stewart, J. H., and Carlson, J. E. Geologic map of Nevada:, 1978.

Tucker, B. E., King, J. L., Hatzfeld, D., and Nersesov, I. L., 1984, Observations of hard-rock site effects: Bulletin of the Seismological Society of America, **74**, no. 1, 121–136.

Wernicke, B., Axen, G. J., and Snow, J. K., 1988, Basin and Range extensional tectonics at the latitude of Las Vegas, Nevada: Geological Society of America Bulletin, **100**, 1738–1757.

DISTRIBUTION:

3 Bechtel Nevada NLV075
ATTN:
Bob White
Michael O'Connor
Dick Ivy
P.O. Box 98521
Las Vegas, NV 89193-8521

1 Jolie Coleman
2201 S. Arrow Court
Pahrump, NV 89048

1 Defense Threat Reduction Agency
ATTN: Dr. Byron Ristvet
1680 Texas Street SE
Kirtland AFB, NM 87117-5669

1 Ivars Gals
3010 Pebble Beach Drive
Pahrump, NV 89048

1 Paul Hernandez
4321 W. Jesse Street
Pahrump, NV 89048

4 Lawrence Livermore National Laboratory
ATTN:
Dr. Karla Hagans, L-149
Dr. Artie Rodgers, Jr., L-205
Dr. Dave McCallen, L-631
Dr. Norman Burkhardt, L-638
P.O. Box 808
Livermore, CA 94551-0808

1 Los Alamos National Laboratory
ATTN: Dr. Frank Cverna
P.O. Box 1663
Los Alamos, NM 87545-001

1 Mr. and Mrs. Jody Maeder
3402 E. Jennifer Street
Pahrump, NV 89061

2 University of Nevada
ATTN:
Dr. John Louie
Dr. Ken Smith
Seismological Lab MS 174
1664 North Virginia Street
Reno, NV 89557

1 University of Nevada, Las Vegas
ATTN: Dr. Catherine Snelson
Geoscience Department
4505 Maryland Parkway
Box 454010
Las Vegas, NV 89154-4010

1 Elida Vargas
1891 Jeane Avenue
Pahrump, NV 89048

1 MS 1190
M. K. Matzen, 1600

1 MS 1168
C. Deeney, 1640

1 MS 1391
D. D. Thomson, 1649

10 MS 1168
R. E. Abbott, 1647

1 MS 1168
L. Chhabildas, 1647

1 MS 0736
M. C. Walck, 6860

2 MS 9018
Central Technical Files, 8944

2 MS 0899
Technical Library, 4536

Sandia National Laboratories